



1 **Laboratory and Field Test and Distinct Element Analysis of Debris Flow**

2 Cheng Yung Ming¹, Li Na¹ and Fung Wing Hong Ivan²

3
4 Department of Civil and Environmental Engineering, The Hong Kong Polytechnic
5 University, Hong Kong¹

6 Department of Architecture and Civil Engineering, City University of Hong Kong²

7
8 **Abstract**

9 Natural as well as fill slopes are commonly found in Hong Kong, China and many other
10 countries, and slope failures with the subsequent debris flows have caused serious loss of lives
11 and properties in the past till now. There are various processes and features associated with
12 debris flow for which the engineers need to know so as to design for the precautionary measures.
13 In this study, experiments on flume tests, friction tests, deposition tests, rebound tests have been
14 carried out for different sizes of balls to determine the parameters required for modelling of
15 debris flow tests. Different materials and sizes of balls are used in the flume tests, and various
16 flow pattern and segregation phenomenon are noticed in the tests. Distinct element (DEM) debris
17 flow modeling are also carried out to model the flow process. It is found that for simple cases,
18 the flow process can be modelled reasonably well by DEM which is crucial for engineers to
19 determine the pattern and impact of the debris flow. The single material and multiple material
20 laboratory tests and numerical simulations can provide further insight into the debris flow
21 process for which only limited field test data can be obtained in general. From the laboratory
22 tests, large scale field tests and numerical simulations, it is also found that the particle size will
23 be the most critical factor in the segregation process during debris flow. It is also found from the
24 laboratory tests and numerical simulations that a jump in the flume can help to reduce the final
25 velocity of the debris flow which is useful for practical purposes.

26
27 Keywords: flume test, field test, balls, debris flow, distinct element, flow process

28
29 **1- Introduction**

30 The terrain of Hong Kong is hilly. Many slopes (fill, cut and natural slopes) and roads are
31 formed to cope with the rapid development of Hong Kong, China and many other developed
32 cities. Hong Kong has a high rainfall, with an annual average of 2300mm which falls mostly in
33 summer between May and September. The stability of man-made and natural slopes is of major
34 concern to the Government and the public. Landslides and subsequent debris flows have caused
35 loss of life and significant amount of property damage in the past. In Hong Kong, for the 50



36 years after 1947, and more than 470 people died due to slope failures and debris flow associated
37 with man-made cut slopes, fill slopes and retaining walls. The Hong Kong Government has spent
38 lots of efforts and money in stabilizing slopes after the serious debris flows in 1972. Even though
39 the risk to the community has been greatly reduced since 1977, on average about 300 slope
40 failure incidents are still reported every year. Although only small amount of incidents can
41 threaten life and property, block the roads and disrupt the lives of the community, engineers still
42 need to pay the attention to slope stability and the subsequent debris flow.

43 There are many reported serious slope failures and debris flow problems in China in the recent
44 ten years, due to the significant amount of constructions and inadequate stabilization to many
45 temporary or permanent fill or natural slopes. The destructive power of large scale debris flow is
46 well known, and the prevention of slope instability, reduction of debris flow destructive power
47 by the use of rigid, flexible barrier or other means are well practiced in many countries. There
48 are many cases where the slopes fail with subsequent debris flows in Hong Kong and China,
49 which have created various serious problems. Based on a conservative estimate, over 60
50 countries in the world have faced the problems of debris flow over the years. In 4-5 November
51 1993, over 800 debris flows were reported in Hong Kong, though most of the flows are small
52 scale in nature. To reduce the impact due to debris flow, both rigid and flexible barrier are
53 adopted in Hong Kong. With reference to Fig.1, the debris flows in Hong Kong and China have
54 created traffic problems, loss of lives and properties, and currently there are many active research
55 works in the area of debris flow in Hong Kong and China. The research works include three-
56 dimensional slope stability analysis, debris flow process, impact loads on flexible and rigid
57 barriers and others. An example on three-dimensional Morgenstern-Price slope stability analysis
58 using 16000 columns has been carried out by Cheng in 2016/2017 which is shown in Fig.2. The
59 analysis of the non-spherical surface is achieved by the use of Nurbs function as discussed by
60 Cheng et al. (2005), and Nurbs representation is a popular method as adopted in many 3D cad
61 programs. Upon the determination of the critical failure mass, and the flow path of the soil can
62 be estimated from a distinct element analysis using the method as discussed by Cheng et al.
63 (2015). The slope failure and the subsequent debris flow as shown in Fig.2 is finally protected by
64 the use of three levels of flexible barrier against the future potential debris flow.

65



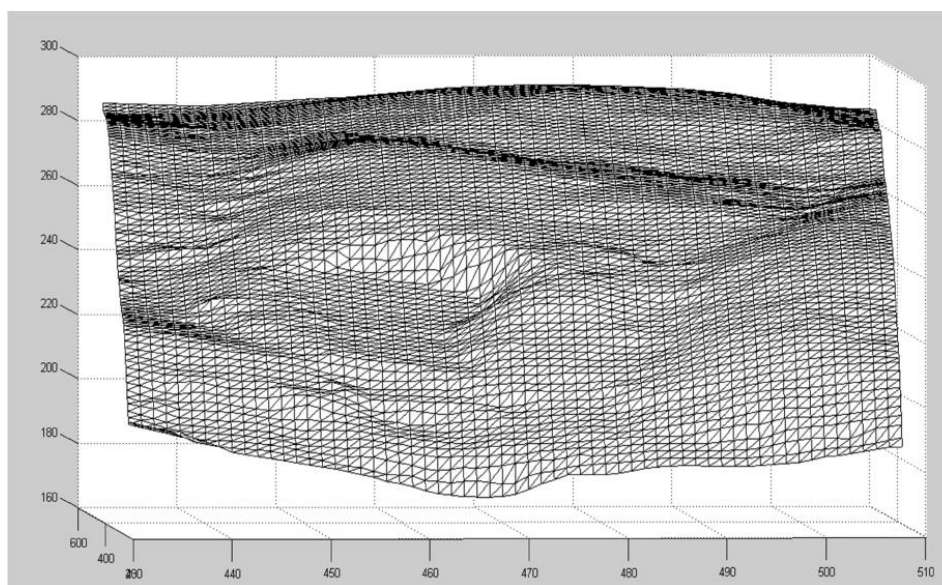
66

67

(a)

(b)

68 Fig.1 Representative debris flow in Hong Kong and Shenzhen, China (a) Tsing Shan debris flow
69 in 1990; (b) debris flow in Shenzhen 2015.



70

71 Fig.2 A three-dimensional slope stability analysis for a slope in Hong Kong (the triangulation
72 represent the geometry as defined by the GIS information)

73

74 Debris flow has some fundamental difficulties in the physical tests as well as numerical analysis.
75 In general, various particles sizes will be present in a flow, and the debris mix is usually far from
76 uniform in composition. For physical tests, it is difficulty to apply a representative debris flow



77 mix, and the flow process is further complicated by the presence of water. For numerical
78 simulation, it is virtually impossible to accommodate too much particles in a model, ranging
79 from a very small particle size to cobbles or even boulder in the extreme range. Even if such a
80 numerical model can be established, there will be serious numerical problems if the particles
81 sizes differ too much in the system. Debris flow can be induced from gravity, driven by fluid
82 dynamic or from both factors. The classification of debris has been given by Varnes (1978), and
83 later modified by Furuya (1980), Ohyagi (1985), Pierson and Costa (1987), Coussot and Meunier
84 (1996), Cruden and Varnes (1996), Hung et al. (2001), Takahashi (2001, 2006) and others. A
85 detailed theoretical treatment of dry granular debris flow similar to some of the single material
86 tests in the present study has been given by Takahashi (2014) and will not be repeated here. In
87 this study, we will concentrate mainly on the action of gravity, while the effects of water is under
88 study by the authors.

89 Many scientists have carried out debris flow analysis. Lo (2004) has compare the different
90 composition of debris flow in landslides in Hong Kong and examine the coarse and fine particle
91 concentration. Hutter et al. (2005) has considered the flow envelopes and the deposition of the
92 debris flow. In year 1991, the U.S. Geological Survey has made a large scale flume for detailed
93 experimental tests on debris flows. The flume is located at the Willamette National Forest, which
94 has a dimension of 1.2 m deep, 2m wide and 95m long. The slope angle of the flume ranges from
95 3 degree to 31 degree, and a removable glass wall is used to initiate the flow. Mizuyama and
96 Uehara (1983) have made a flume which is 20 cm wide and 25m long, and the slope angle ranges
97 from 5 degree to 25 degree. Liu (1996) has made a 18 cm depth, 16 cm width and 150 cm length
98 flume in Yunnan, China, and the flume inclination can be adjusted from 10 to 34 degrees. Lin
99 (2009) has made a 20 cm width 8m length flume with a 2.2 m width 3 m length catchment. There
100 are also various flume tests that have been carried out by various researchers in Hong Kong and
101 many other countries. Laboratory and large scale field flume tests have also been carried out by
102 the authors which will be discussed later.

103 During the transportation period, segregation occurs when debris starts to flow. Iverson (1997)
104 studied the factors that influence the segregation process. He found that particle size has a great
105 effect on the segregation process, and debris with larger particle size move upward while fine
106 particles go downwards. This phenomenon is the opposite of “normal grading” in which the finer
107 particles are found at the upper layers in the lake or river and large particles rest at the bottom.
108 The main reason for the segregation is kinetic sieving, and finer particle can go through the gaps
109 between particles more easily than the larger particle. Large particles can also be found at the
110 front of the flow because of the relatively high velocity of the larger particles at the upper layer,
111 compared with the finer particles with lower velocity at the lower layer. When a stable contact
112 network for large particle is formed at the free surface, the segregation cease to occur and the
113 balls finally deposit at the catchment area.

114 In order to predict and simulate the motion of debris flow, Voellmy (1955) and others combined
115 the point-mass and hydraulic model together. They proposed that the force resisting motion



116 consist of two parts, one is basal frictional force which obey the Coulomb-type friction law, and
117 another one is the turbulent hydrodynamic resistance force resulting from the viscosity of the
118 fluid. Savage and Hutter (1989) derived the depth average equations which are able to predict the
119 flow height and longitudinal velocity in the curvilinear coordinate system (ξ, η) . The first
120 governing equation based on mass balance is given as

$$121 \quad \frac{\partial h}{\partial t} + \frac{\partial hu}{\partial \xi} = 0 \quad (1)$$

122 where t is the time, h is the flow depth, u is the longitudinal velocity. The second equation is
123 derived from momentum balance as

$$124 \quad \frac{d}{dt} = \frac{\partial}{\partial t} + \frac{\partial}{\partial \xi} u = \sin \zeta - s \quad (u)(\cos \zeta + \lambda u^2) \tan \delta - \varepsilon k_a \quad \cos \zeta \frac{\partial h}{\partial \xi} \quad (2)$$

125 where ζ is the local inclination angle, k is the curvature of the base, λ is the curvature-ordering
126 parameter, ε is the aspect ratio, k_a is the earth pressure coefficient. Based on the depth
127 averaged equation, Hungr (1995) introduced the 2D dynamic analysis model from which a
128 complete and practicable numerical model was proposed. After that, a three-dimensional (3D)
129 dynamic analysis through the smoothed particle hydrodynamics theory was proposed by
130 McDougall and Hungr (2004). Recently, a 3D mobility model which include the evolution of
131 pore water pressure was introduced by Iverson and George (2016).

132 For distinct element modeling of debris flow, Jiang et al. (2003) has studied the methods of
133 generations of ball in PFC2D (Cundall 1971, 1988, Cundall and Hart 1992, Cundall and Strack
134 1979), namely the expansion method and isotropic compression method. Zohdi (2007), Halsey
135 and Mahta (2002) have discussed about the physics of granular flow; the contact model and the
136 limit of the friction coefficient. Sullivan (2011) has also compared between the theory and
137 computation in distinct element analysis.

138 In the present study, basic dry granular flow experiments will be conducted under different
139 conditions using glass and rubber balls for a basic study on the flow process and segregation.
140 Both glass and rubber balls of different diameters have been used in the tests, and combination of
141 different size and materials have also been tried in the tests for the illustration of the segregation
142 problem. The experimental results are also analyzed by distinct element analysis using program
143 PFC2D. The tests are performed at relatively simple condition so that the basic problem of flow
144 and segregation can be studied easily. It should also be mentioned that more than 10 ten
145 thousands photos are taken from the laboratory and field tests, and such amount of information
146 cannot be fed into a paper. In views of that, only representative intermediate photos which are
147 used for illustration are given in the present paper, while some of the observed phenomena are
148 simply described without the support of the photos.

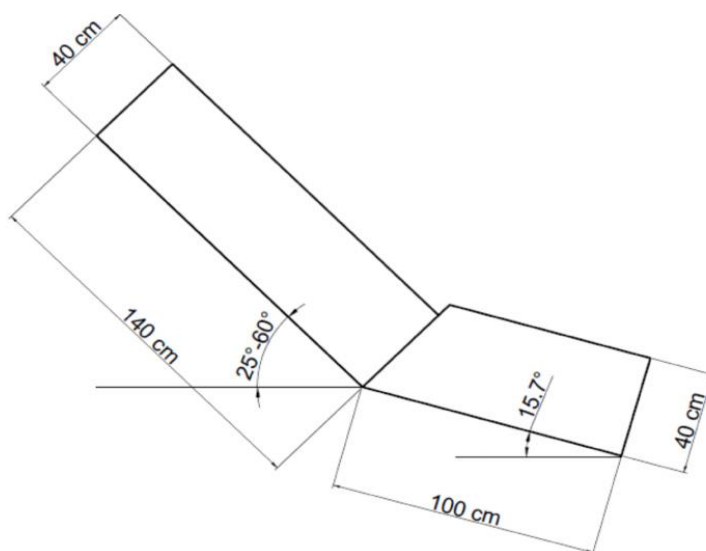
149

150 **2. Physical flume modeling of debris flow**



151 **2.1 Instrumentation and Test Material**

152 To enhance the knowledge on the debris flow mechanism, many laboratory and large scale field
153 tests have been carried out by the authors. The laboratory model is about 1.5m long and 1.3m
154 high (adjustable). The flume in the laboratory is made of polystyrene and is designed to be
155 flexible, and the angle of inclination can be adjusted if necessary. The flume model is 40cm
156 depth, 40 cm width, 140 cm length of upper flume and 100 cm for the lower flume with a 60 x
157 60 catchment area at the bottom. Fig. 3 and Fig 4 show the schematic design of flume and flume
158 model in the laboratory tests. In order to record the motion of the particles, two high speed
159 cameras are adopted. The first one is mounted on the upper flume and the second one is fixed to
160 the bottom flume. In the laboratory tests, different sizes of glass beads and rubber beads are used
161 to replace the use of sand, and this simplification can help to assess the effects of shape and
162 material on the segregation process. In the large scale field test, real sand is used. For the
163 material parameters, the dynamic friction angle is measured by using tilting test (Pudasaini &
164 Hutter (2007), Mancarella & Hungr (2010)). The property of the glass and rubber beads are
165 determined experimentally, and the details are given in Table 1.

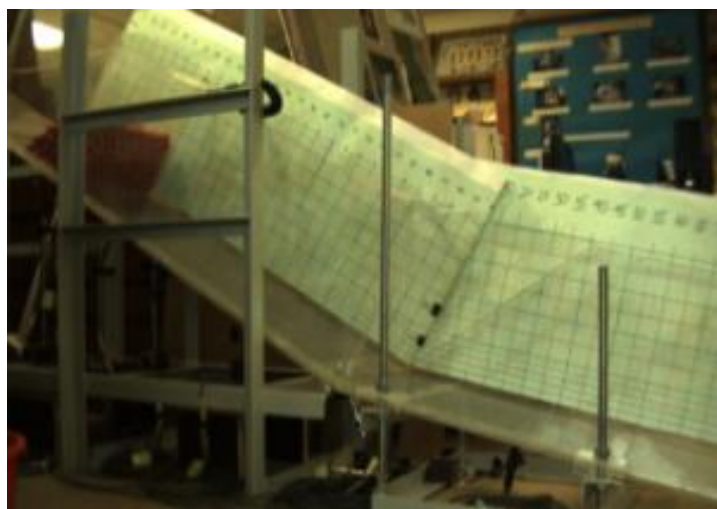


166

167

Fig.3 Schematic Design of Flume

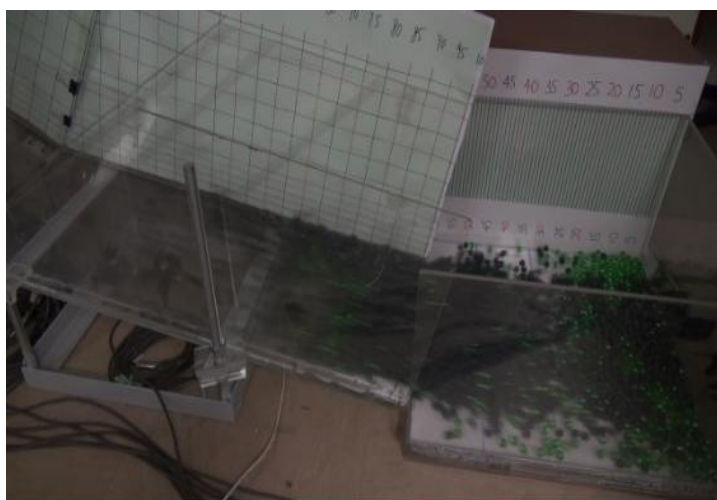
168



169

170

Fig.4 Flume model in laboratory



171

172

Fig 5. Flume model with a small jump in laboratory



173

174 Fig.6a Transparent glass



Fig.6b Blue glass ball



175

176 Fig.6c Green glass ball



Fig.6d White plastic ball



177

178 Fig.6e Red plastic ball



Fig.6f Black plastic ball

179

180 Table 1. The properties for the glass balls and plastic balls in laboratory debris flow test



Plastic	D(mm)	Average Weight	Density (kg/ m ³)	External Friction Coefficient	Internal Friction Coefficient
White	50	105.35	1609.64	0.781	0.547
Red	30	23.382	1653.97	0.630	0.429
Black	15	2.862	1619.56	0.222	0.365
Glass	D(mm)	Average Weight	Density (kg/ m ³)	External Friction Coefficient	Internal Friction Coefficient
Transparent	40	78.686	2348.11	0.102	/
Blue	25	21.121	2581.64	0.053	/
Green	16	5.744	2678.28	0.104	/

181

182 2.2 Test Programme

183 In the present study, the angle of the flume in laboratory is kept to be 45 degree. The effect of the
 184 slope inclination will hence not be investigated in this study (to be covered by another paper
 185 later). Totally 68 laboratory tests have been carried out. The 68 tests are divided into two groups:
 186 the first group of tests were conducted on the flume with a small jump, and the other group of
 187 tests were carried out on the flume without a jump. Such a jump is also commonly adopted in
 188 Hong Kong, and this helps to lower the velocity of the debris (for small scale flow). Fig 5 shows
 189 the flume in laboratory with a small jump. The effects of the particle size and the flowing mass
 190 are also studied through the use of balls with different diameter, mass and combination of
 191 different balls. Table 2 shows only some of the test programme. Test 1 to test 48 belong to the
 192 first tests group with a small flume jump. Test 1 to test 6 were carried out by using six different
 193 kinds of balls separately with the same mass of 10 kg. The mass of the balls is then changed to
 194 13.55kg and the above tests are repeated again (for test 7 to 10). In order to study the segregation
 195 process for test 11 to 40, two kinds of balls with different diameters were combined together, and
 196 for the same purpose in test 40 to test 48, three kinds of balls were combined together. Test 49 to
 197 test 68 belong to the group without a small flume jump. Same as the first group of tests with a
 198 small flume jump, test 49 to test 55 were carried out for same material but different sizes of balls.



199 In test 56 to test 63, combinations of two kinds of balls were tried. The last five tests were the
 200 combination of three kinds of balls.

201

202 Table 2. Test Programme

Flume with a small jump					
One kind of balls	Test Number		Flow Mass		Balls
	1		10 Kg		G(Transparent)
	2		10 Kg		P(White)
	7		13.55Kg		G(Green)
	8		13.55Kg		P(Red)
Two kinds of balls	Test Number		Top Layer		Bottom Layer
	11		P(White)		P(Red)
	26		G(Trans)		P(White)
Three kinds of balls	Test Number	Top Layer	Middle Layer	Bottom Layer	
	41	P(White)	P(Red)	P(Black)	
	45	G(Trans)	P(Red)	P(Black)	

203

Flume without a small jump					
One kind of balls	Test Number		Flow Mass		Balls
	49		10 Kg		G(Transparent)
	50		10 Kg		G(Blue)
Two kinds of balls	Test Number		Top Layer		Bottom Layer
	55		P(White)		P(Black)
	56		G(Trans)		P(Black)
Three kinds of balls	Test Number	Top Layer	Middle Layer	Bottom Layer	
	67	G(Trans)	P(Red)	P(Black)	
	68	G(Trans)	P(Red)	G(Green)	

204 P: P refers to plastic balls, G: G refers to glass beads

205

206 **2.3 Test procedure and test results**

207 Test materials with different particle size combinations (single type of balls to multiple types of
 208 balls) were put into the container which is on the top of the flume. Figure 7 shows the flow
 209 pattern of single type dry granular material flowing along the flume. The video captured by high
 210 speed camera can show this process clearly. When the gate of the container was pulled up, the
 211 front part of flow mass become loose and start to flow along the upper flume under the action of
 212 gravity, while the latter part of flow mass followed behind. Flow mass elongated when it moved



213 forward, and the shape of flow front is wedge-like type. At the moment when the particles
214 reached the bottom of the flume, the velocity direction of the balls changed because of the angle
215 difference between the upper flume and the lower flume. During the transportation period, a
216 large amount of potential energy of the initial flow mass was transferred to momentum energy
217 accompanying by energy dissipation through the grain collision and friction. Particles at the front
218 of the flow reflected back when they impacted on the wall of deposition zone and collided with
219 the subsequent particles immediately, which consumed the residual momentum energy of flow
220 particles. Finally all the particles rested in the deposition zone.

221 In reality, there are sediments and water in a debris flow. The effect of water is complicated, and
222 will not be studied in the present work. The grain size distribution is usually not uniform as in
223 the present laboratory tests. Consequently, a good understanding of the particle flow under a
224 mixture of ball sizes is important. Particle size is a vital parameter for the good understanding of
225 multi-size particle flow because it not only has an effect on the flow dynamic, but also influence
226 the energy attenuation during the whole flow process. What's more, the tilting test that is
227 mentioned above demonstrates that the dynamic friction angle depends on the particle size,
228 specifically, larger particle size will has smaller dynamic friction angle while smaller particle
229 size will has larger dynamic friction angle. The flow pattern of multi-size particle flow is more
230 complicated compared with the single size particle flow.

231 Figure 8 shows the flow pattern of multi-size particle flow. Segregation occurred when the
232 combined particles started flowing along the flume. Figure 8a demonstrates the flow pattern of
233 multi-size particle flow composing of white and black plastic balls. The diameter of the white
234 plastic ball is much larger than the black plastic ball as shown in Table 1. From the video
235 captured by the high speed camera, it is easy to observe that during the transportation period,
236 white plastic balls flowed on the upper layer while black plastic balls stayed at the bottom layer.
237 This phenomenon is consistent with the segregation theory of Savage et al. (1988). Besides, it is
238 not difficult to find that white plastic ball always stayed at the front of the flow where the
239 velocity was the highest, in other word, the velocities of the white plastic balls with relative
240 larger diameters are higher than the black plastic balls. Besides, at the upper layer where larger
241 white plastic balls are located, the inertial force dominated the flow dynamic and the energy
242 dissipation was less than that of the lower layer where the flow motion is mainly controlled by
243 the contact forces. For the forgoing reasons, it can be seen that large particle size leads to higher
244 velocity during the flow.

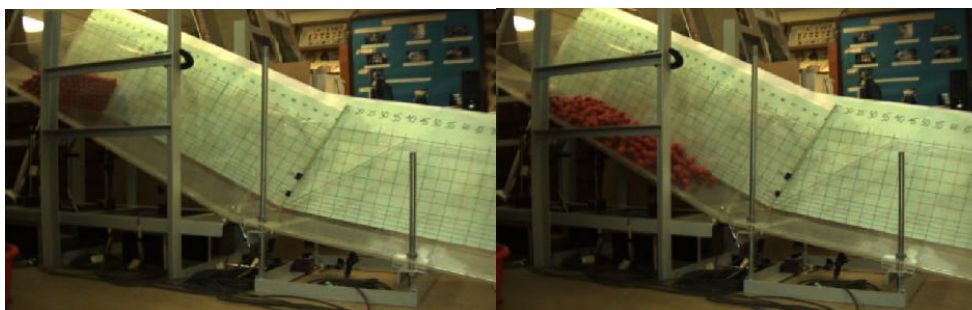
245 Figure 8b shows the flow pattern of multi-size material composing of green glass balls and black
246 plastic balls. The diameter of green glass ball is similar to the diameter of black plastic ball,
247 while the density of green glass ball is almost two times larger than black plastic ball. In the
248 upper container, green glass balls were put statically at the top of the black plastic balls. After
249 pulling up the door, the black plastic balls flowed out firstly at the beginning and stayed at the
250 bottom layer due to the arrangement of the initial position of balls in the container, and then
251 green glass balls quickly moved downwards under the action of gravity, which leads to the fact



252 that green glass balls at the upper layer were replaced by black plastic balls subsequently. When
253 the black plastic balls form a stable contact network at the upper layer of the flow, the position
254 transition or segregation process stopped. In this case, the difference of particle sizes between
255 two kinds of balls is not obvious, and segregation was initiated due to the density difference only.
256 During the segregation process in which green glass balls moved downwards and black plastic
257 balls migrated upwards, the momentums of these two kinds of balls were transferred to each
258 other at neighbor location, therefore green glass balls and black plastic balls arrived at the
259 catchment area almost at the same time, while for the test in which balls were arranged in an
260 opposite order (black plastic balls at top and green glass balls at bottom), the green glass balls
261 move faster and deposit earlier at catchment area compared with the black plastic balls due to the
262 smaller dynamic friction angle as well as the larger kinetic energy of the green glass balls.

263 Similar to the above two figures, Figure 7c shows the flow pattern of transparent glass balls and
264 black plastic balls. In this case, both the density and particle size of the transparent glass balls are
265 larger than that of the black plastic balls. As shown in high speed camera video, during the flow
266 process, the transparent glass balls flow upwards and move faster in comparison with the black
267 plastic balls. Hence, although the density of the transparent glass balls is larger than the black
268 plastic balls, the transparent glass balls still stay at the upper layer of the granular flow due to
269 their relatively large particle sizes, which means that particle size has greater contribution for the
270 segregation process than density in the analysis of debris flow.

271



272

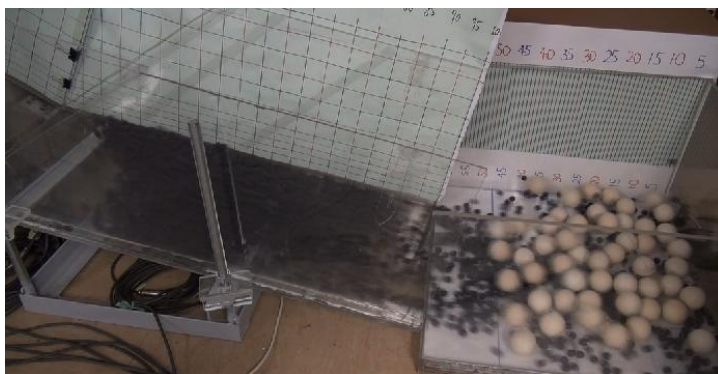


273



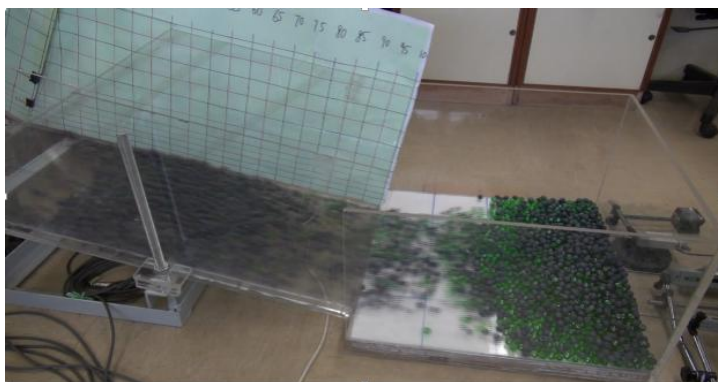
274 Fig. 7. Flow pattern of mono-size particle flow in physical model

275



276

277 a) The influence of particle size on segregation process



278

279 b) The influence of density on segregation process



280



281 c) The influence of particle size and density on the segregation process

282 Fig. 8. Flow pattern of multi-size particle flow

283

284 3. Numerical Modeling of debris flow

285 3.1 Model generation

286 Previous model tests by Chan (2001) for the runout were calibrated by the Dan model, where the
287 problem of segregation and flume jump were not considered. In general, the results are in
288 agreement with those from Rickenmann (in Jacobs and Hungr 2005). For the present studies
289 where multi-size particles are considered, the use of the simple Dan model is insufficient. The
290 laboratory tests in the present study are modelled using the distinct element method in this study,
291 which is more appropriate for the large deformation and separation phenomenon during the
292 transportation process. Once the appropriate numerical model is established, the numerical
293 technique will be extended to the field tests for which natural sand is adopted. In this paper
294 commercial program PFC2D using DEM has been adopted to implement the numerical
295 simulation of dry granular flow. Totally, there are five different methods of model generation in
296 PFC2D program, and based on the consideration time requirement, the rain method was adopted
297 finally. The parameters used in the numerical simulation are the micro-properties which are
298 difficult to be determined. Benchmark tests have been carried out in order to calibrate the micro-
299 mechanical properties of the dry granular material. Some of the micro-parameters of the balls are
300 determined through changing their values so that the macroscopic behaviors in numerical
301 simulation are consistent with that in physical test. The detailed micro-properties of the balls are
302 shown in Table 3. The diameters of the particles in the numerical analysis are the same as that
303 used in the physical tests.

304

305 Table 3. Microscopic parameter of the balls for debris flow analysis

Balls	Ball stiffness (N/m ²)	Ball damp	Ball density (kg/m ³)	Ball friction	Wall friction	Wall stiffness (N/m ²)
Red plastic ball	2.36e9	0.4	1250	0.462	0.1	1.11e11
Black plastic ball	7e8	0.2	1250	0.1	0.1	1.11e11
Blue glass ball	7e10	0.3	2500	0.1	0.1	1.11e11



Green glass ball	7e10	0.2	2500	0.1	0.1	1.11e11
------------------	------	-----	------	-----	-----	---------

306

307

308 3.2 Numerical test results

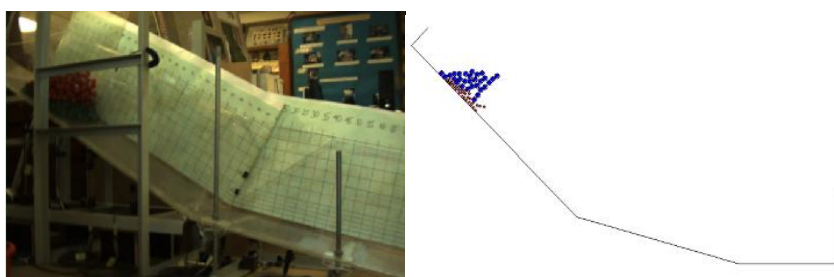
309 A detailed comparison of the particle flow pattern modeled by the physical tests and discrete
310 element analysis is shown in Figure 9. Figure 9a shows the physical test in which both the red
311 plastic balls and green glass balls were used (too many test results are available, and only
312 selected results are used for illustration in this paper). Large blue balls and small red balls in the
313 numerical model represent the actual red plastic balls and green glass balls in the physical model
314 tests respectively. A full-scale numerical simulation is rare to be conducted for discrete element
315 analysis due to the limitation of the computer resource, but this is considered to be necessary and
316 acceptable for the present study. Figure 9b shows the numerical results of the flow pattern of the
317 multi-size particles. Particles start to flow along the flume after the initiation of the flow. During
318 the flow process, the flow mass became longer under the action of shear force. Particles moved
319 apart from each other and pushed other particles forwards. During this process, the momentums
320 of the balls were exchanged and transferred to other balls at the neighbor locations. The flow
321 velocity keep increasing until the front of the flow hit on the wall of the deposition zone. When
322 the kinetic energy of the balls was exhausted, the balls eventually ceased to move at the
323 catchment area. Figure 10 shows the flow pattern of multi-size balls flows composing of black
324 plastic balls and green glass balls of which the diameter are relative smaller than the other balls
325 as considered in the present paper. A pronounced Saltation was observed as balls flowed,
326 implying that the collisional character of the flow mass where the savage number is larger than
327 0.1 (if the savage number is smaller than 0.1, the flow belongs to frictional flow, Iverson 1997).
328 Savage number is the ratio between inertial force and frictional force. The comparison between
329 Figure 10, and Figure 9b indicates that the larger the ball size, the more collisional the flow
330 mechanism would be. As a result, the inertial forces dominate the flow dynamic compared with
331 the frictional forces in the present tests. Furthermore, the balls at the upper region of the flow
332 associated with higher velocity had more collisions and moved freely compared with that at the
333 bottom region. The balls at the lower region were compacted with lower flow velocities. By
334 comparison, the numerical simulation results of the flow pattern have a very good agreement
335 with the physical test results when the micro-parameters were selected suitably.

336 As shown in Figure 9b and Figure 10, segregation was also observed in the numerical model
337 after the dry granular balls started to move. In Figure 9b, it was evident that the blue balls with
338 larger ball size moved upwards and forwards, while the red balls with smaller ball size went to
339 the lower layer and stayed at the rear of the flow, which was consistent with the results in the
340 physical model tests. Smaller particles are more likely to move through the void between the
341 larger particles, and this will in turn squeeze the large particles to the upper layer of the flow.
342 Because of the momentum exchange between the balls and the flow mass dilation resulting from
343 the shear deformation, a dispersive pressure was caused which result in larger dry granular balls

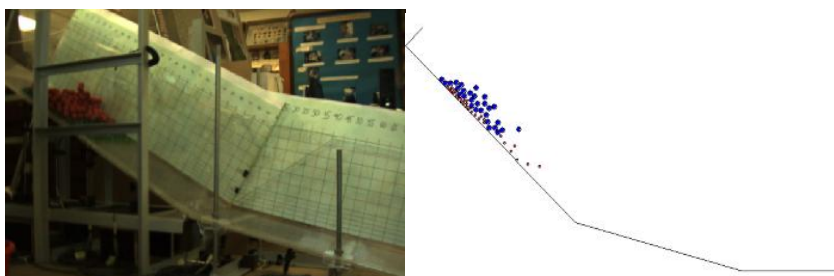


344 moved faster than the finer particles and went upwards, and lead to the results that larger balls
345 flowed to the upper layers where the shear strain is low and accumulated at the front of the flow,
346 while the finer balls tend to moved downwards and accumulated at the bottom of the flow
347 (Takahashi (1981)). Besides, the difference of the ball size induce an unbalance forces on the
348 balls which restrict the vertical movement of the balls, and this will affects the flow segregation
349 in the vertical direction. What's more, the density difference between the balls the in numerical
350 model is another factor that influence the segregation process. Particles with lower density are
351 more likely to rise to the free surface while particles with higher density are more likely to
352 segregate to the bottom of the flow. From Figure 5b, it can be noticed that it is easily for the red
353 balls with larger density traveled through the gap generated by the shear deformation and
354 squeezed the particle with smaller density up to the upper flowing layer. The balls with higher
355 density at the bottom pushed the balls with smaller density forward. It is worth to mention that
356 from the simulation results, the velocities of the blue balls at free surface is the largest, which
357 result in that the balls with large size migrated to the front of the flow. The segregation
358 mechanism simulated in the numerical model is in consistent with what is aforementioned in the
359 physical model tests. Ashwood and Hungr (2016), Choi et al. (2014), Choi et al. (2015), Kwan
360 (2012), Lo (2000), Ng et al. (2014), Ng et al. (2017) have investigated the impact forces on the
361 barrier which is however not investigated in the present study.

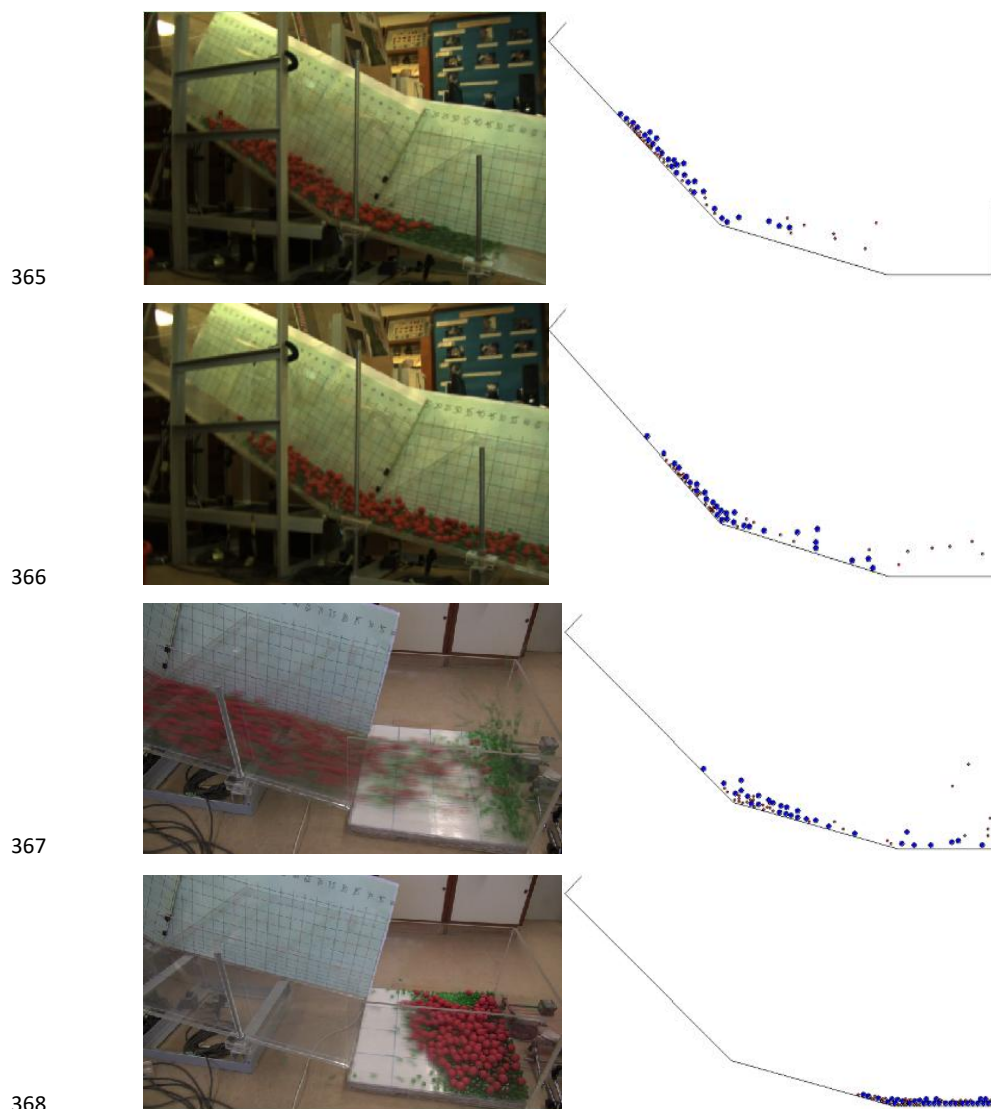
362



363



364



365

366

367

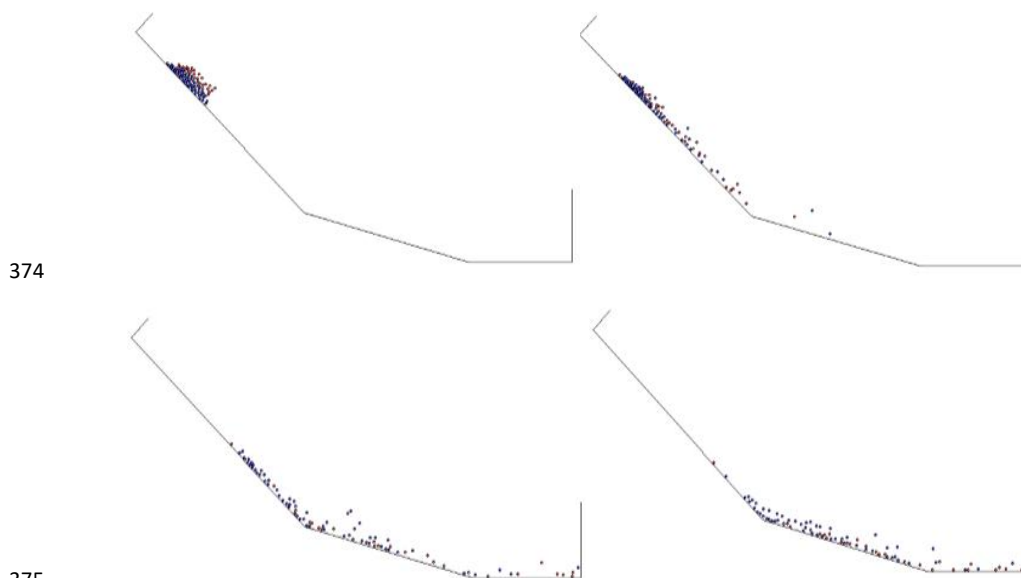
368

369 Fig. 9a. Flow pattern of multi-size
370 balls flow in physical test

Fig. 9. Flow pattern of multi-size
balls flow in numerical test

371 Fig. 9. Flow Pattern of multi-size particle flow composing of red plastic balls and green
372 glass balls

373



374

375

376

377 Figure 10. Flow Pattern of multi-size particle flow composing of black plastic

378 balls and green glass balls

379

380 3.3 The effect of the flume jump

381 Figure 11 shows the numerical results of the flow pattern of the blue glass balls flowing on the
382 flume with or without a jump. The flow pattern of the blue glass balls flowing on the flume
383 without a jump in the numerical model is almost the same as the flow pattern of the red plastic
384 balls in the physical tests aforementioned. From the comparison of the flow pattern between
385 Figure 11a and Figure 11b, an important phenomenon was observed. The run up height of the
386 balls flowing on the flume with a jump is obviously lower than the run up height of the particles
387 flowing on the flume without a jump, which indicates that flume jump is able to facilitate the
388 process of energy attenuation and thereby has a good effect on suppressing the run up height of
389 debris flow. This is also the reason why this jump is commonly adopted in Hong Kong for
390 locations with potential small scale debris flow.

391 Figure 12 exhibits the velocity of the blue glass balls at different time step. Black line represent
392 the maximum velocity of the blue glass balls with 10Kg weight flowing on the flume without a
393 jump at different time step, while the red line represent the same kind of balls with 13.55Kg
394 weight on the flume with a jump. The comparison of the velocities at point A and point B
395 indicates that the peak velocity of the balls flowing on the flume with a jump is pronouncedly

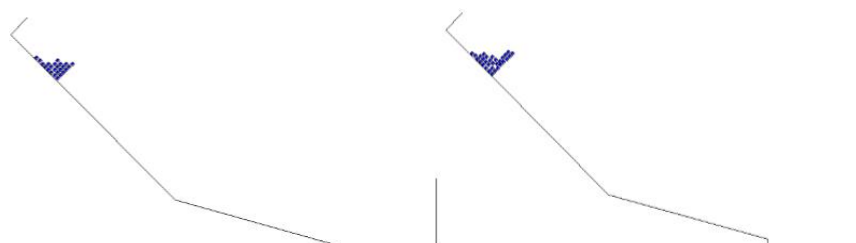


396 smaller than that on the flume without a jump, and the peak speeds of the balls on the flume with
397 a jump were achieved earlier than balls on the flume without a jump. It is worth to mention that
398 the velocity of the balls is independent of the mass of the test material, except that at the peak
399 period.

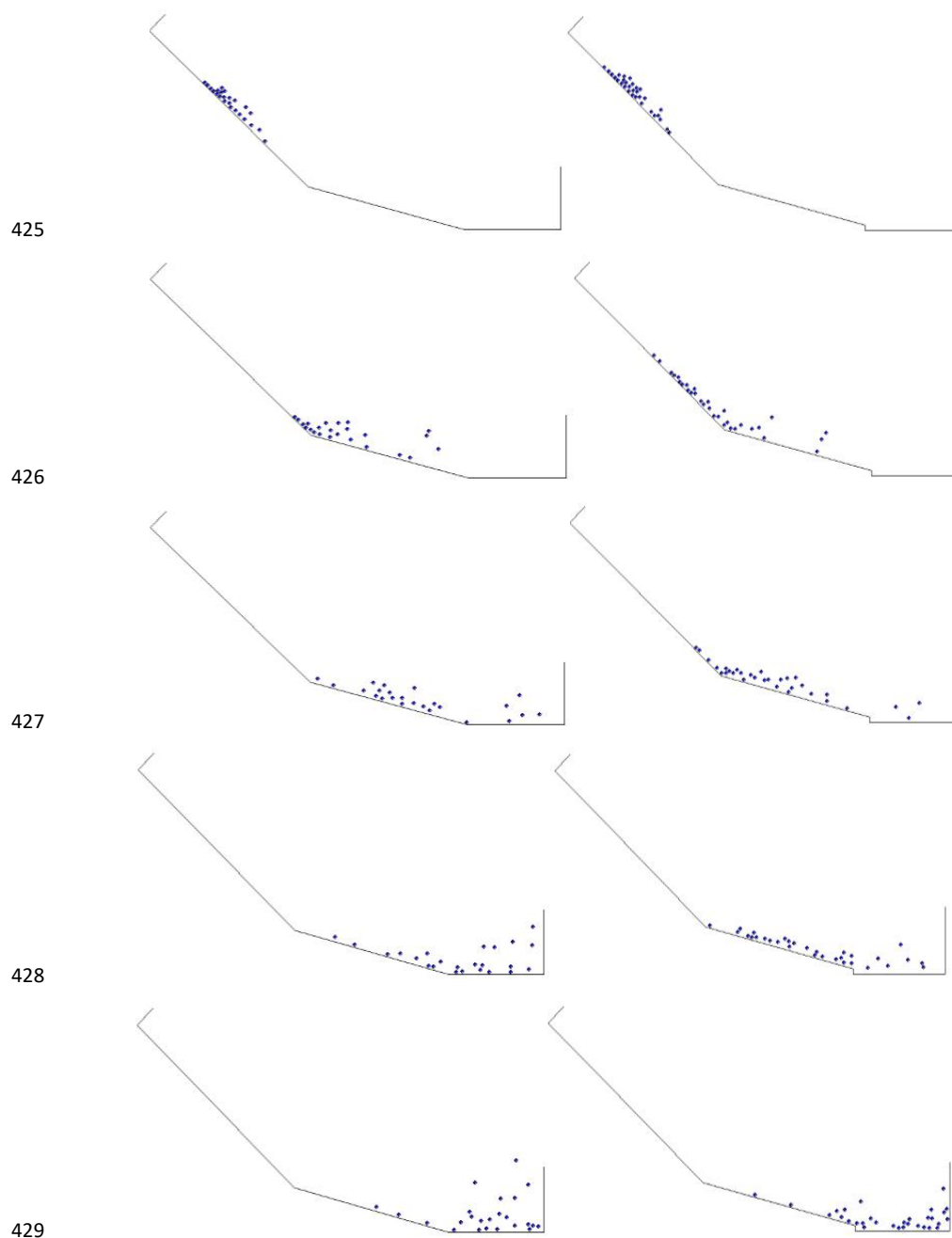
400 Figure 13 shows the velocity profile of mono-size particles (blue glass balls) along the flume
401 with or without a flume jump. The length of the velocity vector represents the speed of the
402 particles. From Figure 13, it can be noticed that the front flow velocities are the largest compared
403 with the velocities of the particles at the rear of the flow. When these particles approached the
404 lower part of the flume, the velocity directions changed due to the difference of the flume angles.
405 This is in good agreement with the laboratory results mentioned above. Figure 13b shows that
406 the velocity of mono-size particles on the flume with a jump increased after the initial state. The
407 largest flow velocity was achieved at the moment when these particles intend to jump into the
408 deposition zone. The directions of flow velocities changed and the speed of particles decrease
409 as soon as they fell into the deposition zone. As with those particles moving on the flume with a
410 jump, the velocity of the particles flowing along the flume without a jump increased when they
411 approached the deposition zone, however, the velocity of these particles kept increasing when
412 they flowed into the deposition area and the peak speed was achieved just before the moment
413 when they reached the boundary of the deposition area. When the granular front impacted on the
414 wall of the deposition area, these particles at the front of the flow reflect back and collide with
415 the following particles, and that is the moment when the flow speed decelerated.

416 According to Figure 12 and 13, the peak velocity of the balls on the flume with a jump achieved
417 before they impacted on the wall of deposition zone compared with that without a jump, which is
418 meaningful to the engineers because the flume jump can effectively reduce the impact force on
419 the barrier. Besides, the jump of the flume is capable of reducing the peak velocity of the dry
420 granular particle flow as well. To sum up flume jump, plays a vital role in attenuating debris
421 flow, therefore, flume jump is recommended to be applied in the design of debris flow barrier
422 (which is actually adopted in Hong Kong and other places).

423



424





430

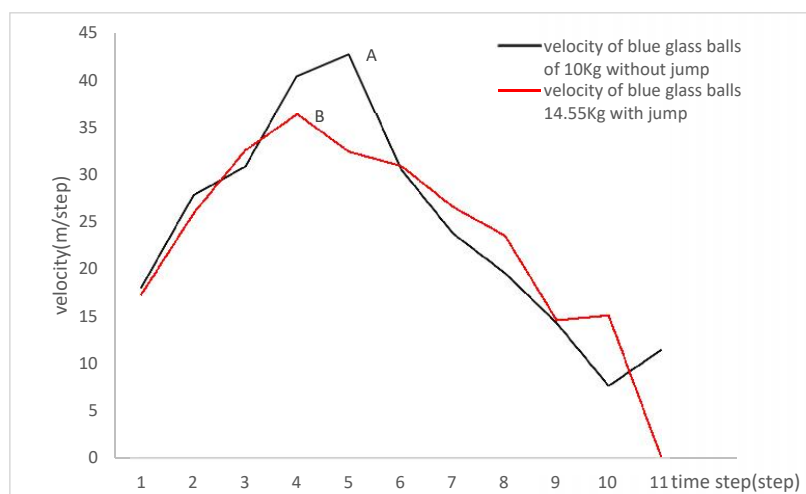
431

432 Fig. 11a. Flow pattern of blue glass balls
433 flowing along the flume without jump

432 Fig. 11b. Flow pattern of blue glass balls
433 flowing along the flume with jump

434 Fig. 11. Flow pattern of blue glass balls flowing on the flume with or without a jump

435

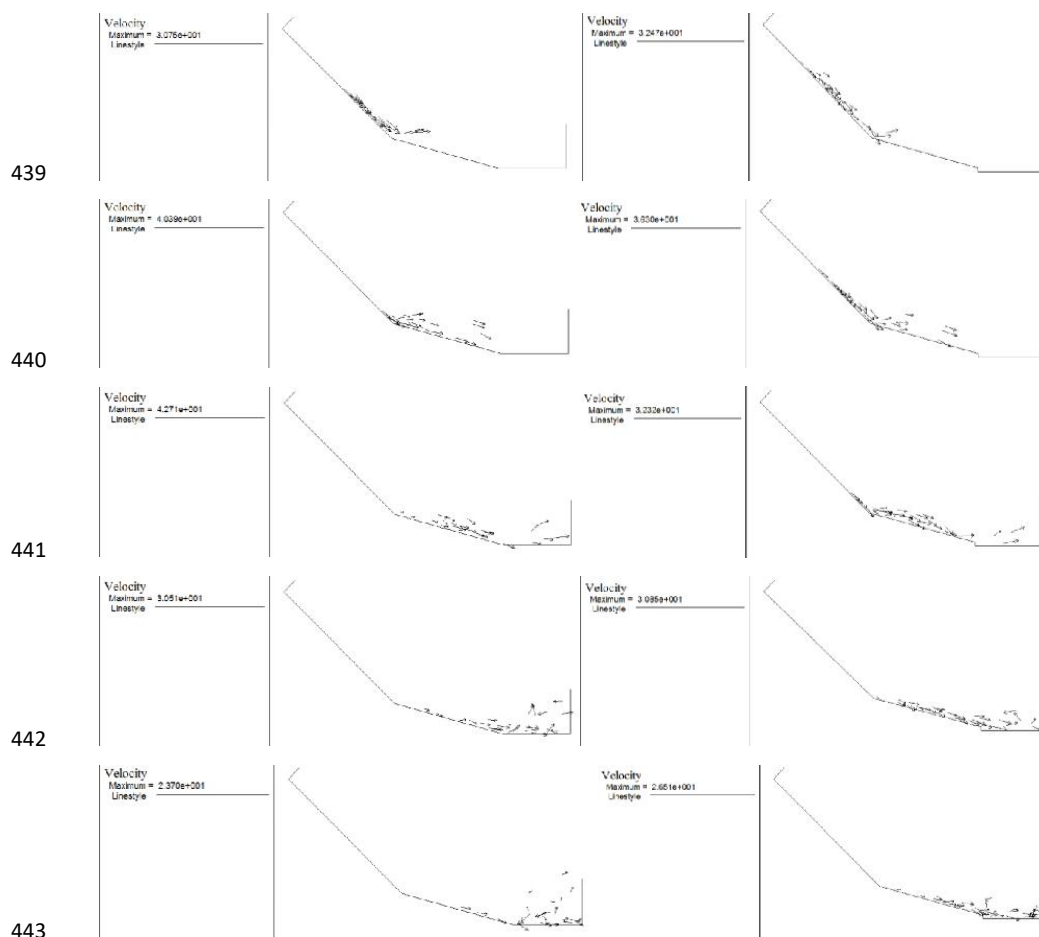


436

437

437 Fig. 12. Maximum velocity of blue glass balls in numerical model

438



444 Fig. 13a. Velocity profile of balls on the flume without a jump
445
446 Fig. 13b. Velocity profile of balls on the flume with jump
447

448 Fig. 13. Velocity profile of blue glass balls in numerical model

449 5. Large scale field tests

450 After the laboratory studies using a 1.5m long flume and glass/rubber balls, the authors have
451 carried out a large scale flume test which is shown in Fig.14. The flume is about 6m long, and 5
452 types of sand as shown in Fig. 15 are used in the field tests. The particle size within each type is
relatively uniform, and they ranged from 1-3mm, 3-5mm, 5-7mm, 7-8mm and above 8mm. The



453 friction angles for the 5 types of sand as determined from the deposition tests as shown in
454 Fig.15b are given by 28° , 30.3° , 29.1° , 31.5° and 33.7° respectively.



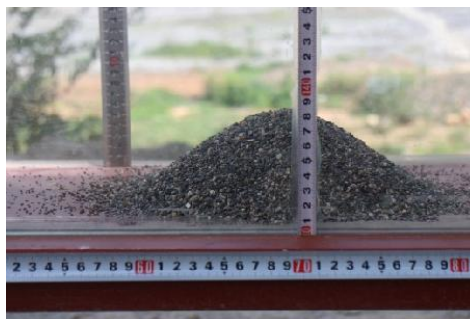
455

456 Fig.14 Large scale flume for field test



457

458 Fig.15a Sand used for debris flow tests



459 Fig.15b Deposition tests for sand

459

460 A series of tests with single, double and triple types of sand have been carried out, and only some
461 of the results are shown in this paper for comparisons with the laboratory tests. As shown in
462 Fig.16, the final deposition profile using type 1 (1-3mm) and type 4 (7-8mm) sands is shown. It
463 is noticed that the coarse grain sand move to the top of the flow, which are illustrated by Fig.17a
464 to 17c. Such results comply well with the laboratory studies. The control tests using coarse and
465 finer sands are shown in Fig.18. A closer look into the difference between Fig. 18a and Fig.16 is
466 the profile at the rear can reveal an important difference. For debris flow with 2 types of
467 materials, the difference in the height of deposit for the first meter as measured from the left is
468 greater than that for the test with single material (true for all single sand tests). Such
469 phenomenon can be attributed to the effect of the difference in the velocity flow between type 1
470 and 4 material, and type 1 material deposit at the bottom during the flow. Based on the field tests,
471 the importance of the particle size during the segregation process as derived from the laboratory
472 tests can be further verified.

473



474

475 Fig.16 Final deposition after the debris flow for two materials (coarse and fine)



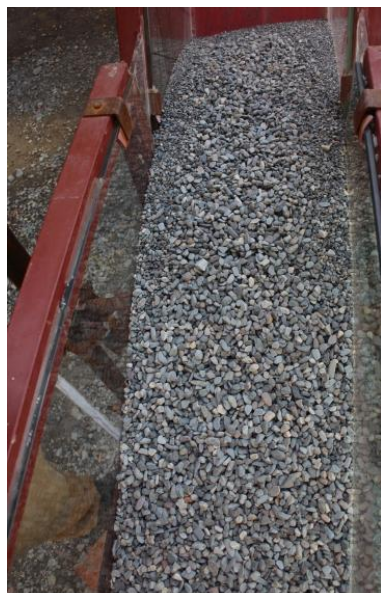
476

477 Fig.17 a Deposition at the rear of the deposit



478

Fig.17b Deposition at the front of the deposit



479

480 Fig.17c Front view of the deposition (2 materials)

481



482

483 Fig.18a Front view of the deposition (type 4 material) Fig.18b Close up view of the deposition

484

485 With reference to Fig.19, it is clear that the formation of the flow front, flow head, channelized
486 flow and levee from the present field test is very similar to that by Johnson et al. (2012). The
487 surface trajectories of the particles by Johnson et al. (2012) are also captured by the high speed
488 camera in the present laboratory and field tests. A coarse enriched surface layer has been
489 obtained by Johnson et al. (2012), and such phenomena are also obtained from the laboratory and
490 field tests and is clearly illustrated in Fig.17. Iverson (1997) has also found similar segregation



491 from the debris flow at Oregon (1996). It should be noted that for all the debris flow tests in the
492 present study, such segregation phenomenon is always obtained, as long as there are more than 1
493 materials in the problems.



494

495 Fig.19 Front of the runout

496 **6. Discussion**

497 Laboratory tests were carried with numerical simulations through distinct element method to
498 study the flow pattern of dry granular flow. The study is important for the basic understanding of
499 the debris flow segregation problem and the importance of providing a jump in the flume or in
500 the actual protective measures. For the present tests, the flume base is even and smooth which
501 result in relative small dynamic frictional angle and less energy attenuation compared with the
502 debris flow. Besides, the surfaces of the glass and plastic balls used in the experiments are
503 regular and smooth, while for debris flow occurring in nature the debris materials are irregular
504 and rough, which cause the dynamic internal frictional shear force between real scale debris flow
505 particles are relatively large and hence the run up height is lower. As a consequence, it is a
506 conservative method of present tests to study the flow pattern of debris flow. Such arrangement
507 is necessary so as to clearly identify the contribution of particle size distribution in the
508 segregation process.

509

510 Physical tests were conducted to study the flow pattern of mono as well as multiple size particle
511 flows. In general, the results from the present study comply well with those from the literature.
512 Test results indicate that flow mass elongated under the action of shear force during the particles
513 flowed on the flume. For multi-size particles with different particle sizes, segregation always
514 occurs. Particles with larger diameters migrated upward and small particles moved downwards



515 because particles with smaller diameter can go through the gap between the larger particles. In
516 addition, the density of the particle is another factor that play a role in the segregation process.
517 Under the action of gravity, particles with higher density moved downwards faster and other
518 particles with lower density were squeezed up. For the real scale debris flow, the debris material
519 ranges from clay and silt to boulders while the differences in the densities between different
520 types of particles are relatively small, hence particles size will be the most dominant factor which
521 influence the segregation process. Top view from the high speed camera indicates that the
522 velocities of the large particles are higher than the velocities of the small particles. Granular
523 particles with larger particles sizes travelled to the front of the flow where the velocities are
524 higher. Larger particle size is observed to lead to a higher velocity. Such results are also in
525 general agreement with the results by Takahashi (1980).

526 For the flow pattern of dry granular particles simulated through distinct element method, the
527 simulation results of flow pattern are almost the same as the physical tests. Berger (2016), Chen
528 and Lee (2000), Ghilardi et al. (2001) also obtained a reasonably well numerical modeling of the
529 flow process for relatively simple flow problem which support the use of numerical analysis for
530 the debris flow problem. In the present numerical model, a pronounced segregation process was
531 observed as well, which comply well with many previous studies by Gray et al. (2003),
532 Hákonardóttir et al. (2003), Iverson (1997), Johnson et al. (2012) and many others. Large
533 particles went upwards while small particles went downwards. From the velocity vector figure,
534 the velocities of the particles at upper layer as well as the velocities at the front of the flow were
535 the largest. Savage numbers of the dry granular particles in present tests were larger than 0.1,
536 which represent the collisional character of the flow. The flow behavior was hence more inertial
537 than frictional. Flume jump have a significant influence on the impeding debris flow. When the
538 particles flowed through the jump a large quantity of kinetic energy were consumed during this
539 process. The peak velocities of particles flowing on the flume with a jump were lower than that
540 without a flume jump. Besides, the peak velocities of the particles on the flume with a jump were
541 achieved earlier, and after that the flow velocity started to decrease, which would make a great
542 contribution for reducing the impact load. The run up height of the particles on the flume with a
543 jump was apparently lower than that without a jump. Thus, flume jump can help to reduce the
544 flow velocity as well as suppress the run up height.

545 Comparing the physical and numerical test results, the macroscopic flow behavior in numerical
546 models are consistent with the physical tests. Through a good selection of the model generation
547 method and micro parameters, the distinct element method can produce a reasonable qualitative
548 simulation of the behavior of dry granular flow for the consideration of the engineers. These
549 results have useful contributions to the better understanding of the debris flow behavior which is
550 not possible for other classical methods.

551

552 **7. Conclusion**

553 In the present study, two important phenomena in debris flow are studied. The first problem is
554 the segregation process which is captured in all the tests in the present studies. The segregation



555 phenomenon can affect the design of the barrier in different ways. The finer materials will be
556 deposited at the bottom of the runout, and the relatively lower permeability of this layer will tend
557 to drive the water level upward (somewhat similar to the perch water table phenomenon). This
558 may increase the destructive power of water. For the design of rigid barrier, the use of a suitable
559 water table will also be crucial to maintain adequate factor of safety of the barrier. Since
560 segregation will occur practically for majority of the debris flow problems, this effect should be
561 well studied and considered in the design of flexible and rigid barriers.

562

563 To reduce the destructive power of the debris, a small jump in the flow channel is sometimes
564 applied in Hong Kong if the site condition allow. In general, the effect of this jump is small, and
565 is effective only for small volume debris flow which is the common case for Hong Kong.
566 Nevertheless, such provision can slightly reduce the destructive power of the debris. It is
567 interesting to note that there is virtually no study about the effect of the jump in the past, and the
568 present work provide some useful pilot works, for which more works may come out in the future.

569

570 **Acknowledgement**

571 The present project is funded from the Research Grants Council of the Hong Kong SAR
572 Government through the project PolyU 152293/16E, and CityU University of Hong Kong
573 Research Project No. 7004631.

574

575 **Reference**

- 576 Ashwood, W., & Hungr, O. (2016). Estimating total resisting force in flexible barrier impacted
577 by a granular avalanche using physical and numerical modeling. *Canadian Geotechnical Journal*,
578 53(10), 1700-1717.
- 579 Berger C. (2016), A comparison of physical and computer-based debris flow modelling of a
580 deflection structure at Illgraben, Switzerland, INTERPRAEVENT 2016, 212-220.
- 581 Chan, C. P. L. (2001). Runout distance of debris flows: experimental and numerical simulations
582 (Doctoral dissertation, The Hong Kong Polytechnic University).
- 583 Chen H. and Lee C.F. (2000), Numerical simulation of debris flow, *Canadian Geotechnical*
584 *Journal*, 37:146-160.
- 585 Cheng Y.M., Liu H.T. and Au S.K. (2005), Location of critical three-dimensional non-spherical
586 failure surface with applications to highway slopes, *Computers and Geotechnics*, no. 32, 387-399.
- 587 Cheng YM, Li N. and Yang XQ (2015), Three Dimensional Slope Stability Problem with a
588 Surcharge Load, *Natural Hazards And Earth System Sciences*, 15(10), 2227-2240.
- 589 Choi, C. E., Au-Yeung, S. C. H., Ng, C. W., & Song, D. (2015). Flume investigation of landslide
590 granular debris and water runup mechanisms. *Géotechnique Letters*, 5(1), 28-32.



- 591 Choi, C. E., Ng, C. W., Song, D., Kwan, J. H. S., Shiu, H. Y. K., Ho, K. K. S., & Koo, R. C. H.
592 (2014). Flume investigation of landslide debris-resisting baffles. *Canadian Geotechnical Journal*,
593 51(5), 540-553.
- 594 Coussot, P. and Meunier, M. (1996), Recognition, classification and mechanical description of
595 debris flows, *Earth-Science Reviews*, 40: 209–227.
- 596 Cruden, D.M. and Varnes, D.J., (1996), *Landslide Types and Processes*, Special Report ,
597 Transportation Research Board, National Academy of Sciences, 247:36-75
- 598 Cundall, P. A. (1971). A computer model for simulating progressive large scale movements in
599 blocky rock systems. In *Proc. Symp. Rock Fracture (ISRM)*, Nancy, France, 129-136.
- 600 Cundall P A. (1988), Formulation of a three-dimensional distinct element model—Part I. A
601 scheme to detect and represent contacts in a system composed of many polyhedral blocks,
602 *International Journal of Rock Mechanics and Mining Sciences & Geomechanics Abstracts*.
603 Pergamon, 25(3): 107-116.
- 604 Cundall, P. A. and Hart, R. D. (1992). Numerical modelling of discontinua. *Engineering*
605 *Computations*, 9(2), 101-113.
- 606 Cundall, P. A. and Strack, O. D. (1979). A discrete numerical model for granular assemblies.
607 *Geotechnique*, 29(1), 47-65.
- 608 Furuya, T., 1980, Landslides and landforms: in *Landslides, slope failures and debris flows*
609 (Takei, A. ed.), Kajima Shuppan, Tokyo, pp.192–230.
- 610 Ghilardi P., Natale L. and Savi F. (2001), Modeling debris flow propagation and deposition,
611 *Phys. Chem. Earth* 9:951-656.
- 612 Gray, J. M. N. T., Tai, Y. C., & Noelle, S. (2003). Shock waves, dead zones and particle-free
613 regions in rapid granular free-surface flows. *Journal of Fluid Mechanics*, 491, 161-181.
- 614 Hákonardóttir, K. M., Hogg, A. J., Batey, J., & Woods, A. W. (2003). Flying avalanches.
615 *Geophysical Research Letters*, 30(23).
- 616 Halsey and Mahta (2002), *Challenges in Granular Physics*, World Scientific
- 617 Hungr, O. (1995), A model for the runout analysis of rapid flow slides, debris flows, and
618 avalanches, *Can. Geotech. J.*, 32, 610–623.
- 619 Hungr O., Evans S.G., Bovis M. and Hutchinson J.N. (2001), Review of the classification of
620 landslides of the flow type, *Environmental and Engineering Geoscience*, VII, 221-238.
- 621 Hutter, K., Wang, Y., & Pudasaini, S. P. (2005). The Savage–Hutter avalanche model: how far
622 can it be pushed? *Philosophical Transactions of the Royal Society of London A: Mathematical,*
623 *Physical and Engineering Sciences*, 363(1832), 1507-1528.



- 624 Iverson, R. M., Reid, M. E., & LaHusen, R. G. (1997). Debris-flow mobilization from landslides
625 1. *Annual Review of Earth and Planetary Sciences*, 25(1), 85-138.
- 626 Iverson, R. M., & LaHusen, R. G. (1989). Dynamic pore-pressure fluctuations in rapidly
627 shearing granular materials. *Science*, 246(4931), 796-800.
- 628 Iverson, R. M., & LaHusen, R. G. (1993). Friction in debris flows: Inferences from large-scale
629 flume experiments. *American Society of Civil Engineers (Ed.), Hydraulic Engineering*, 93.
- 630 Iverson R.M. (1997), The physics of debris flows, *Reviews of Geophysics*, 35(3):245-296.
- 631 Iverson, R.M., and George, D.L., (2016), Discussion of “The relation between dilatancy,
632 effective stress and dispersive pressure in granular avalanches” by P. Bartelt and O. Buser, *Acta*
633 *Geotechnica*, 11(6), 1465-1468
- 634 Jakob M. and Hungr O. (2005), *Debris flow hazards and related phenomena*, Springer Praxis.
- 635 Jiang, M., J. Konrad, and S. Leroueil (2003). An efficient technique for generating homogeneous
636 specimens for DEM studies, *Computers and Geotechnics* 30, 579–597.
- 637 Johnson A.M. (1996), A model for grain flow and debris flow, U.S. Department of the Interior
638 U.S. Geological Survey, Open-file-report 96-728.
- 639 Johnson C.G., Kokelaar B.P., Iverson R.M., Logan M., LaHusen R.G. and Gray J.M.N.T. (2012),
640 Grain-size segregation and levee formation in geophysical mass flows, *Journal of Geophysical*
641 *Research*, 117, F01032.
- 642 Kesseli, J. E. (1943). Disintegrating soil slips of the Coast Ranges of Central California. *The*
643 *Journal of Geology*, 51(5), 342-352.
- 644 Kwan, J. S. H. (2012). Supplementary technical guidance on design of rigid debris-resisting
645 barriers. Geotechnical Engineering Office, HKSAR. GEO Report, (270).
- 646 Li K.H. (2013), *Laboratory debris flow flume test*, Hong Kong Polytechnic University.
- 647 Lin, D. G., Hsu, S. Y., & Chang, K. T. (2009). Numerical simulations of flow motion and
648 deposition characteristics of granular debris flows. *Natural hazards*, 50(3), 623-650.
- 649 Liu, X. (1996). Size of a debris flow deposition: model experiment approach. *Environmental*
650 *Geology*, 28(2), 70-77.
- 651 Lo, D. O. K. (2000). Review of natural terrain landslide debris resisting barrier design. HKSAR:
652 GEO, Report no. 104.
- 653 Lo, K. H. (2004). Theoretical simulations of debris flow and their applications to hazard
654 mapping using GIS (Doctoral dissertation, The Hong Kong Polytechnic University).
- 655 Major, J. J. (1997). Depositional processes in large-scale debris-flow experiments. *The Journal*
656 *of Geology*, 105(3), 345-366.



- 657 Mancarella D. and Hungr O. (2010), Analysis of run-up of granular avalanches against steep,
658 adverse slopes and protective barriers, *Canadian Geotechnical Journal*, 2010, 47(8): 827-841
- 659 McDougall and Hungr (2004), A model for the analysis of rapid landslide motion across three-
660 dimensional terrain, *Canadian Geotechnical Journal*, 41(6): 1084-1097
- 661 Mizuyama, T., Uehara.S., (1983), Experimental study of the depositional process of debris flows.
662 *Trans. Jpn. Geomorph. Union* 4, 39-64.
- 663 Ng, C. W. W., Choi, C. E., Kwan, J. S. H., Koo, R. C. H., Shiu, H. Y. K., & Ho, K. K. S. (2014).
664 Effects of baffle transverse blockage on landslide debris impedance. *Procedia Earth and*
665 *Planetary Science*, 9, 3-13.
- 666 Ng, C. W. W., Choi, C. E., Liu, L. H. D., Wang, Y., Song, D., & Yang, N. (2017). Influence of
667 particle size on the mechanism of dry granular run-up on a rigid barrier. *Géotechnique Letters*,
668 7(1), 79-89.
- 669 Ohyagi, N., 1985, Definition and classification of sediment hazards: in Prediction and
670 countermeasures of sediment hazards (Japanese Soc.Soil Mech. Foundation Eng. ed.), Japanese
671 Soc. Soil Mech. Foundation Eng., Tokyo: 5–15.
- 672 Pierson, T.C. and Costa, J.E., 1987, A rheologic classification of subaerial sediment-water flows:
673 in Debris flows/avalanches: process, recognition, and mitigation (Costa, J.E. and Wieczorek, G.F.
674 eds.), *Rev. Eng. Geol.*, 7, *Geolo. Soc. Am*: 1–12.
- 675 Pudasaini S.P., Wang Y. and Hutter K. (2005), Modelling debris flows down general channels,
676 *Natural Hazards And Earth System Sciences*, 5, 799-819.
- 677 Pudasaini & Hutter (2007), *Avalanche Dynamics, Dynamics of Rapid Flows of Dense Granular*
678 *Avalanches*, Springer Verlag.
- 679 Rodine, J. D., Johnson, A. M., & Rich, E. I. (1974). Analysis of the mobilization of debris flows.
680 STANFORD UNIV CALIF DEPT OF GEOLOGY.
- 681 Rodolfo, K. S., Umbal, J. V., Alonso, R. A., Remotigue, C. T., Paladio-Melosantos, M. L.,
682 Salvador, J. H. and Miller, Y. (1996). Two years of lahars on the western flank of Mount
683 Pinatubo: Initiation, flow processes, deposits, and attendant geomorphic and hydraulic changes.
684 Fire and mud: eruptions and lahars of Mount Pinatubo, Philippines, 989-1013.
- 685 Mizuyama, T., & Uehara, S. (1983). Experimental study of the depositional process of debris
686 flows. *Japanese Geomorphological Union*, 4(1), 49-63.
- 687 Savage, S. B. and Hutter, K. (1989), The motion of a finite mass of granular material down a
688 rough incline, *J. Fluid Mech.*, 199, 177–215.
- 689 Savage S.B. and Lun C.K.K. (1988), Particle size segregation in inclined chute flow of dry
690 cohesionless granular soils, *J. Fluid Mech.*, 199, 177-215.
- 691 Sullivan, C. (2011). *Particulate discrete element modelling*. Taylor & Francis.



- 692 Takahashi, T. (1981). Debris flow. *Annual review of fluid mechanics*, 13(1), 57-77.
- 693 Takahashi, T., (2001), Mechanics and simulation of snow avalanches, pyroclastic flows and
694 debris flows, *Spec. Publ., Int. Ass. Sediment*, 31: 11–43.
- 695 Takahashi, T., (2006), Mechanisms of sediment runoff and countermeasures for sediment
696 hazards, Kinmirai Sha.
- 697 Takahashi T. (2014), *Debris Flow - Mechanics, Prediction and Countermeasures*, 2nd edition,
698 CRC Press.
- 699 Varnes, D.J., (1978), Slope movement types and processes: in *Landslides analysis and control*
700 (Scguster, R.L and Krizek, R.J. eds.), *NAS Sp. Rep.* 176: 11–33.
- 701 Voellmy, A. (1955), Über die Zerstörungskraft von Lawinen. *Schweizerische Bauzeitung* 73,
702 159–162, 212–217, 246–249, 280–285. In German.
- 703 Yamashiki Y., Mohd Remy Rozainy M.A.Z.c, Matsumotod T., Takahashie T. and Takarabc K.
704 (2013), Particle Routing Segregation of Debris Flow Mechanisms Near the Erodible Bed,
705 *Procedia APCBEE*, 527-534.
- 706 Zohdi, T. I. (2007), P-wave induced energy and damage distribution in agglomerated granules
707 Modelling and simulation in materials science and engineering. 15, S435-S448.
- 708 Zhou G.D., Law R.P.H. & Ng C.W.W. (2009), The mechanisms of debris flow: a preliminary
709 study, *Proceedings of the 17th International Conference on Soil Mechanics and Geotechnical*
710 *Engineering*, 1570-1573.